AGU PUBLICATIONS

Geochemistry, Geophysics, Geosystems

TECHNICAL REPORTS: DATA

10.1002/2017GC007274

Key Points:
- A new bathymetric compilation of the southwest Indian Ocean
- The most comprehensive map of the southwest Indian Ocean including new high-resolution multibeam data

Supporting Information:
- Figure S1
- Figure S2
- Figure S3
- Table S1

Correspondence to:
B. Dorschel,
Boris.Dorschel@awi.de

Citation:
Dorschel, B., Jensen, L., Arndt, J. E., Brummer, G.-J., de Haas, H., Fielies, A., et al. (2018). The southwest Indian Ocean Bathymetric Compilation (swIOBC). *Geochemistry, Geophysics, Geosystems*, *19*, 968–976. https://doi.org/10.1002/2017GC007274

Received 4 OCT 2017
Accepted 18 FEB 2018
Accepted article online 26 FEB 2018
Published online 12 MAR 2018

© 2018. The Authors.
This is an open access article under the terms of the Creative Commons Attribution-NonCommercial-NoDerivs License, which permits use and distribution in any medium, provided the original work is properly cited, the use is non-commercial and no modifications or adaptations are made.

The Southwest Indian Ocean Bathymetric Compilation (swIOBC)

B. Dorschel[1], L. Jensen[1], J. E. Arndt[1], G.-J. Brummer[2,3], H. de Haas[2], A. Fielies[4], D. Franke[5], W. Jokat[1], R. Krocker[1], D. Kroon[6], J. Pätzold[7], R. R. Schneider[8], V. Spieß[9], H. Stollhofen[10], G. Uenzelmann-Neben[1], M. Watkeys[11], and E. Wiles[11]

[1]Alfred Wegener Institute Helmholtz Centre for Polar and Marine Research, Bremerhaven, Germany, [2]NIOZ – Royal Netherlands Institute for Sea Research and Utrecht University, Texel, The Netherlands, [3]Department of Earth Sciences, Faculty of Earth and Life Sciences, VU University Amsterdam, HV Amsterdam, The Netherlands, [4]Petroleum Agency South Africa, Cape Town, South Africa, [5]Federal Institute for Geosciences and Natural Resources, Hannover, Germany, [6]School of GeoSciences, Grant Institute, University of Edinburgh, Edinburgh, UK, [7]MARUM – Center for Marine Environmental Sciences, University of Bremen, Bremen, Germany, [8]Institute for Geosciences, Kiel University, Kiel, Germany, [9]Geoscience Department, University Bremen, Bremen, Germany, [10]Geo-Center of Northern Bavaria, Friedrich-Alexander University of Erlangen-Nuremberg, Erlangen, Germany, [11]Geological Sciences, University of KwaZulu-Natal, Durban, South Africa

Abstract We present a comprehensive regional bathymetric data compilation for the southwest Indian Ocean (swIOBC) covering the area from 4°S to 40°S and 20°E to 45°E with a spatial resolution of 250 m. For this, we used multibeam and singlebeam data as well as data from global bathymetric data compilations. We generated the swIOBC using an iterative approach of manual data cleaning and gridding, accounting for different data qualities and seamless integration of all different kinds of data. In comparison to existing bathymetric charts of this region, the new swIOBC benefits from nearly four times as many data-constrained grid cells and a higher resolution, and thus reveals formerly unseen seabed features. In the central Mozambique Basin a surprising variety of landscapes were discovered. They document a deep reaching influence of the Mozambique Current eddies. Details of the N-S trending Zambezi Channel could be imaged in the central Mozambique Basin.

Plain Language Summary Maps are crucial not only for orientation but also to set scientific processes and local information in a spatial context. For most parts of the ocean seafloor, maps are derived from satellite data with only kilometer resolution. Acoustic depth measurements from ships provide more detailed seafloor information in tens to hundreds of meters resolution. For the southwest Indian Ocean, all available depth soundings from a variety of sources and institutes are combined in one coherent map. Thus, in areas where depth soundings exist, this map shows the seafloor in so-far unknown detail. This detailed map forms the base for subsequent studies of e.g. the direction of ocean currents, geological and biological processes in the southwest Indian Ocean.

1. Introduction

The demand for high-resolution bathymetric grids from local studies to regional compilations has been identified for a variety of marine disciplines. Only on the basis of gridded data sets, it is possible to understand and interpret regional, local, and point data in a spatial context. Due to past and ongoing research activities in the southwest Indian Ocean, a large amount of bathymetric data has accumulated for this area over the past decade forming a critical mass of data for a regional bathymetric compilation. Combined in a coherent data grid, the individual data sets form a comprehensive Digital Bathymetric Model (DBM) (Figure 1) for an area of importance from geological, oceanographical, and climatological perspectives.

Geologically, the southwest Indian Ocean was shaped during the Gondwana breakup that occurred in the southwest Indian Ocean during the Cretaceous with massive magmatism and subsequent rifting (Davies et al., 1995; Eagles & König, 2008; Gaina et al., 2013; Jokat et al., 2003; König & Jokat, 2010; Leinweber et al., 2013; Salman & Abdula, 1995). The Cretaceous evolution of the Mozambique Ridge (also known as Mozambique Plateau according to the GEBCO SubCommittee on Undersea Feature Names) and Agulhas Plateau is

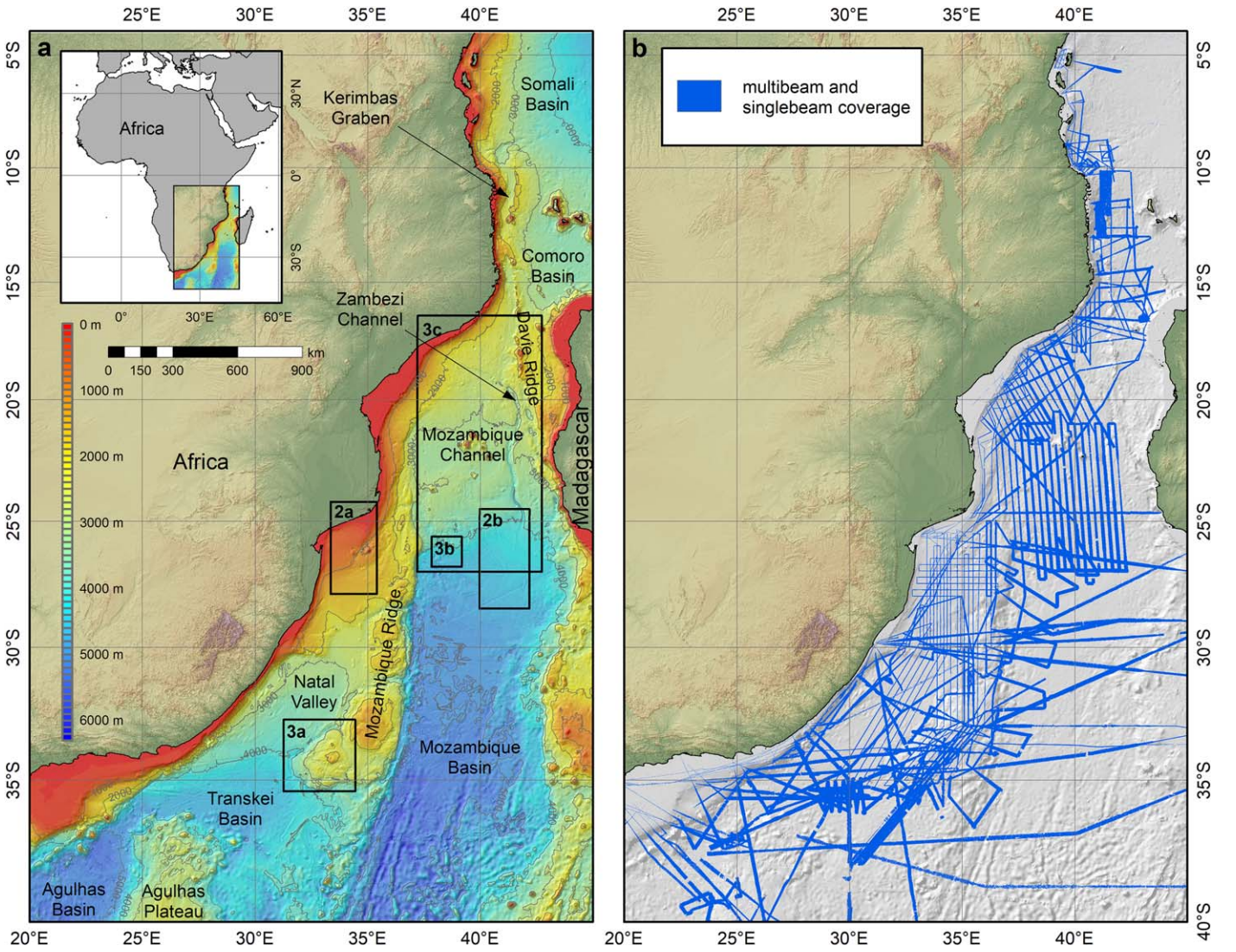

Figure 1. Southwest Indian Ocean Bathymetric Compilation. Figure 1a shows a representation of the swIOBC Version 1.0 Digital Bathymetric Model (DBM) displaying the major plateaus, ridges, and basins. The image is a combination of a hillshade-relief and a bathymetry raster to create a pseudo-3D effect. Rectangles show the extent of Figures 2 and 3. Figure 1b shows the coverage of multibeam and singlebeam data. The multibeam coverage overlay is the Source Identifier (SID) grid of the values of each cell of the swIOBC-DBM. A list and a map of all data sources is available in the supporting information linking each cell of the swIOBC to the identifier (ID) in the SID expedition list. Furthermore, maps showing the differences between the swIOBC-DBM and GEBCO_14 and providing information on the number of soundings per grid cell are provided in the supporting information. The swIOBC-DBM, the SID grid, and supporting grids are available at https://doi.org/10.1594/PANGAEA.880618.

still under debate. Studies present conflicting interpretation of these features as being of oceanic or continental origin (Gohl & Uenzelmann-Neben, 2001; Gohl et al., 2011; König & Jokat, 2010; Parsiegla et al., 2008; Tucholke et al., 1981; Uenzelmann-Neben et al., 1999). Recent geophysical studies (Fischer et al., 2017; König & Jokat, 2010; Parsiegla et al., 2008) support the interpretation of these ridges as large igneous provinces of Cretaceous age associated with the opening of the southwest Indian Ocean. Late Miocene neo-volcanism at the Mozambique Ridge is interpreted as an extension of the western branch of the East African Rift System (Fischer et al., 2017).

Sediments from the African continent in the west have formed deposits on shelves. Canyons often occur as the extension of rivers on the adjacent continental slopes. Erosion, transport, and deposition by various water masses (interacting with large-scale tectonic features) have resulted in the present-day seafloor morphology of the southwest Indian Ocean. Furthermore, sediment waves and contourite drifts are the result

of the interplay of bottom currents with the seafloor (Uenzelmann-Neben, 2001; Uenzelmann-Neben et al., 2007).

At present, the southwest Indian Ocean is an area of dynamic exchange of Atlantic, Indian, and Southern Ocean water masses (de Ruijter et al., 1999; Gordon, 1986; Hood et al., 2017; Lutjeharms, 2006; Lutjeharms & Van Ballegooyen, 1988; Siedler et al., 2009; van Leeuwen et al., 2000). Below the southward flowing surface currents, the pathway of northward flowing meridional deep water masses entering the Indian Ocean follows the topography of the deep ocean basins steered by the ridges and plateaus in the area (Schott & McCreary, 2001; Schott et al., 2002, 2009; Xie et al., 2002).

Maps derived from high-resolution bathymetric data sets are sparse, despite the scientific importance, with the existing maps only allowing for the identification of large morphological structures (e.g., the Agulhas Plateau and the Mozambique Ridge). Sedimentary features such as sediment waves or drifts are too small to be visible in these maps and thus, for comprehensive and in-depth investigations of the southwest Indian Ocean, higher-resolution maps than currently available are necessary.

Research activities in the southwest Indian Ocean during the past three decades have increased the amount of available depth soundings. However, these were scattered in various databases and have not been integrated into a single bathymetric data set. Therefore, we initiated the southwest Indian Ocean Bathymetric Compilation (swIOBC) as a regional mapping project under the auspice of the General Bathymetric Chart of the Oceans (GEBCO) and the parent organizations the Intergovernmental Oceanographic Commission (IOC) of UNESCO and the International Hydrographic Organization (IHO). The swIOBC will be included in future versions of GEBCO and support the Nippon Foundation-GEBCO Seabed 2030 Project (Mayer et al., 2018).

Here, we present the swIOBC Version 1.0 DBM. The swIOBC-DBM has a spatial resolution of 250 m (8.1″) and is based on the WGS84 ellipsoid. It covers an area from 4°S to 40°S and from 20°E to 45°E (Figure 1a) including the passive continental margin of southeast Africa and the adjacent ocean basins. From north to south, this includes the southwest part of the Somali Basin, the Comoro Basin, the Mozambique Channel, the Mozambique Basin, the Natal Valley, the Transkei Basin, and the northern-most part of the Agulhas Basin (Figure 1a). Davie Ridge, Mozambique Ridge, and Agulhas Plateau separate these basins. In the northeast, the study area covers the western parts of Madagascar (Figure 1a). The DBM, the corresponding Source Identifier (SID) grid, and supporting grids are available for download at: https://doi.org/10.1594/PANGAEA.880618.

2. Data and Methods

2.1. Data

The swIOBC V1.0 includes multibeam data from 42 cruises acquired by 8 different institutes. In total, about 1.883 billion multibeam depth-soundings are included in the swIOBC. The majority of the soundings (57.8% of the multibeam data-constrained grid cells in the final swIOBC-DBM) originate from expeditions led by the Alfred Wegener Institute Helmholtz Centre for Polar and Marine Research (AWI). These data were mostly post-processed (corrected for changing sound velocities in the water column but not corrected for tides). Most of these data have not yet been included in other regional or global bathymetric compilations. Another large portion of multibeam data (20.2%) originates from the National Centers for Environmental Information (NCEI), an open access database (https://www.ncei.noaa.gov/) formerly known as National Geospatial Data Center (NGDC). The remaining 22.0% were contributed by the German Bundesamt für Seeschifffahrt und Hydrographie (BSH), the US Naval Oceanographic Office (NAVOCEANO), the Dutch Koninklijk Nederlands Instituut voor Zeeonderzoek (NIOZ), the Petroleum Agency South Africa (PASA), the Institut Français de Recherche pour l'Exploitation de la Mer (IFREMER), and the Japan Agency for Marine-Earth Science and Technology (JAMSTEC). The received data sets were mostly unprocessed raw data (with limited or no meta-data) acquired between June 1993 and April 2014. Because the data sets were recorded over a long time span and on different platforms, the quality of the data was heterogeneous in terms of acquisition system, background data, resolution, accuracy, and documentation (see also the supporting information). These multibeam data form the backbone of the swIOBC database.

In addition to the multibeam data, the swIOBC database contains approximately 135,000 singlebeam soundings. These soundings were downloaded as unprocessed data from the NCEI. In contrast to the

multibeam data, for the singlebeam data metadata were mostly absent. Furthermore, these data were often acquired en-route without quality control and sound velocity corrections. In general, only an average sound velocity of 1,500 ms^{-1} was applied. Furthermore, tides, equipment offsets, drafts, etc. were not taken into account either. This resulted in a lower data quality compared to the multibeam data.

In areas without multibeam or singlebeam coverage, bathymetric information from GEBCO_14 (Weatherall et al., 2015) was used. The GEBCO_14 DBM has a resolution of 30" and incorporates several global and regional bathymetric compilations in which the seafloor topography of areas with no directly measured data was estimated from satellite altimetry (Smith & Sandwell, 1997).

The topography of land areas was derived from the digital elevation model (DEM) of the NASA Shuttle Radar Topographic Mission (SRTM) (Jarvis et al., 2008). This DEM (Version 4) has a spatial resolution of 90 m $\times$ 90 m at the equator. For the swIOBC, the SRTM data were resampled at a resolution of 250 m $\times$ 250 m.

2.2. SwIOBC Database

All multibeam, singlebeam, and gridded data were converted to xyz (longitude, latitude, depth) ascii data for the swIOBC database, In addition, each data point received a source identification (SID) number. The SID number contains information on the type of data and on the platform the data were recorded from. A weight factor for each data point accounted for different data qualities. The data were split into square tiles of 0.9° $\times$ 0.9° to minimize the computing time during gridding. In this way, when data sets were modified, added or removed from the compilation, only specific tiles had to be updated. For each tile, systematic errors and spurious measurements were rejected from the multibeam and singlebeam data with the QPS Fledermaus® software suite. These programs allowed for an efficient and comprehensive area-based data cleaning in 3D-view by integrating all multibeam and singlebeam data sets from a region.

2.3. Data Gridding and DBM Generation

To calculate the swIOBC-DBM, we used a gridding algorithm that handles the different source data qualities in multiple steps. It is similar to the algorithms used for the International Bathymetric Chart of the Arctic Ocean (IBCAO) (Jakobsson et al., 2012) and the International Bathymetric Chart of the Southern Ocean (IBCSO) (Arndt et al., 2013). From high-quality data only (i.e., multibeam data acquired after 2000), the weighted median for 250 m $\times$ 250 m grid cells was calculated. To do so, the depths values were sorted in ascending order and the weighted median was defined as the first depth value where the cumulated sum of the weights assigned to the depth values is $\geq$ 50% of the sum of all weights. Using a weighted median instead of the "standard" median ensured that higher quality soundings (high weight) were preferred over soundings of lower quality in grid cells where data with different qualities were present. From the median data, with the Generic Mapping Tools (GMT) (Wessel et al., 2013) function *nearneighbor*, a grid with a resolution of 250 m $\times$ 250 m was calculated only for grid cells containing high-quality data (N-grid). In addition to the N-grid, a second grid was computed with 1,000 m $\times$ 1,000 m resolution using the weighted median on all available multibeam and singlebeam xyz data as input data. For this grid the GMT *surface* function "continuous curvature splines under tension" (Smith & Wessel, 1990) was used with a tension factor of 0.35. Furthermore, the maximum value was constraint to -1 m to avoid the creation of artificial islands, and the minimum value was constrained to the minimum of the input median data. The resulting grid (S-grid) contained interpolated values for every grid cell, in contrast to the N-grid that only contained values where high-quality data existed.

For the final grid, the S-grid and the N-grid were combined as follows: The S-grid was resampled to 250 m resolution. Grid cells containing no high quality data were assigned the S-grid value v_S. Grid cells containing high quality data were assigned the N-grid value except those located within a transition zone of 500 m adjacent to the N-grid values. In the transition zones, values v_c were calculated as a linear combination of the S-grid and the N-grid value:

$$v_C = \frac{v_S d_S^2 + v_N d_N^2}{\left(d_S^2 + d_N^2\right)}$$

where v_S and v_N are the depth values of the S- and the N-grid, and d_S and d_N are the inverted distances of the grid cell to the outer (d_S) and inner (d_N) edge of the transition zone. This transition avoided abrupt artificial steps in the data set at the edges of the S-grid and the N-grid values. In an iterative process, the

resulting composite grid (C-grid) was examined in Fledermaus and obviously erroneous xyz data leading to erroneous grid cells were identified and rejected. This process was repeated until no coarse errors were obvious in the C-grid any more.

Land data were pasted into the C-grid similar to the combination of the S-grid and the N-grid. However, to prevent that small islands represented only by a few grid cells were forced below water level due to the linear combination within the transition zone, we left all land grid cells unchanged and defined a 500 m buffer zone around the land area. Within this buffer zone, we calculated the depth values by interpolating with a linear nearest distance interpolator.

In a final step, areas containing no sounding data were filled with data from GEBCO_14 (Weatherall et al., 2015), using the same combination algorithm as for the S-grid and the N-grid, but with a larger transition zone of 10 km defined around all existing data (not only around high quality data). However, using the original GEBCO_14 grid lead to undesired artefacts as there are offsets between C-grid values and GEBCO_14 values. Thus, GEBCO_14 was adjusted prior to gap-filling via multiplication with a factor grid, calculated as follows: For every grid cell containing data the factor between the C-grid value and the GEBCO_14 value was calculated. These factors were used as input data for the GMT *surface* algorithm, after applying a 5 km GMT *blockmedian* to suppress small-scale variations. This resulted in a smooth factor grid used to adjust GEBCO_14 depths to measured depths. In areas where GEBCO_14 differed strongly from the C-grid (e.g., flat shelf areas), after careful examination, GEBCO_14 data were excluded and interpolated values were used instead.

3. Results and Discussion

The swIOBC represents the most comprehensive bathymetric compilation for the southwest Indian Ocean (Figure 1a). Compared to GEBCO_14, the coverage of grid cells constrained by depth soundings has increased from 5.5% in GEBCO_14 to 21.3% in the swIOBC-DBM. The improvements are most pronounced in the Transkei Basin, Natal Valley, and Mozambique Ridge. The Kerimbas Graben in the north of the study area (Figure 1a) is fully covered by a multibeam survey (Figure 1b). In addition, wide spaced multibeam

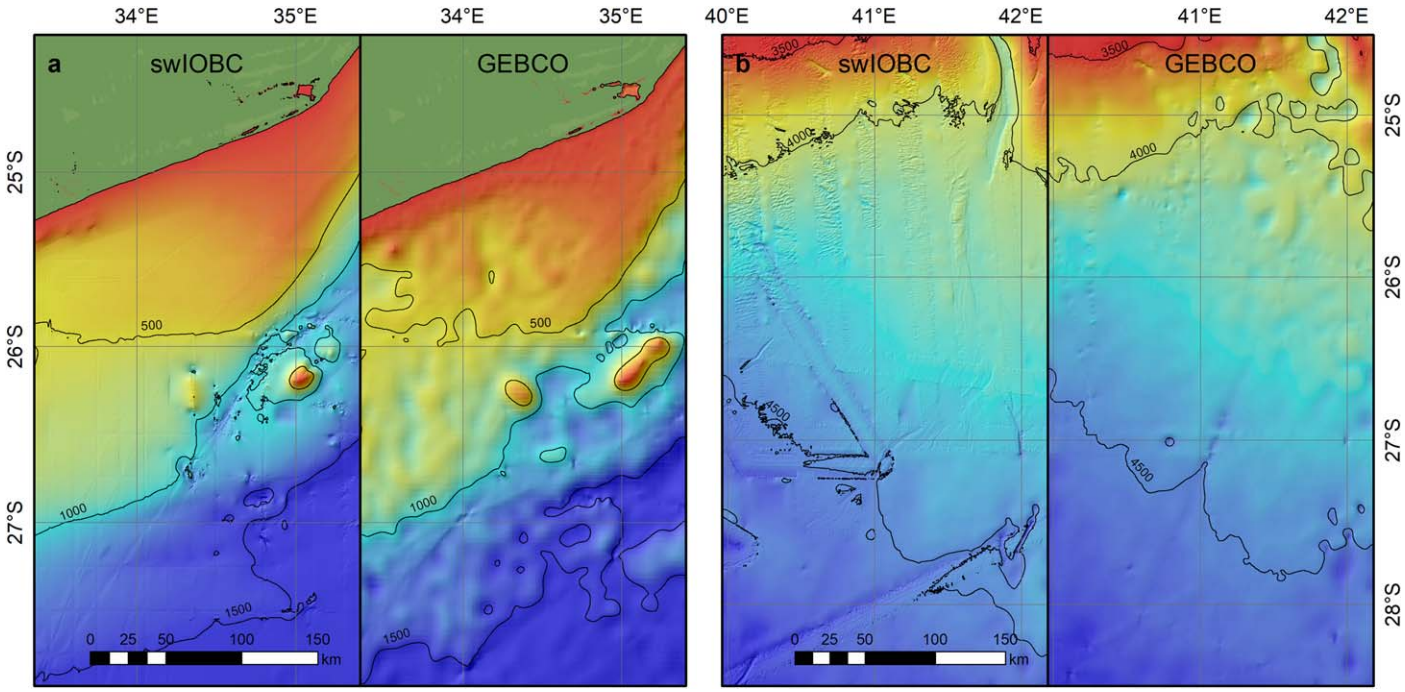

Figure 2. Comparison of the swIOBC and the GEBCO_14 DBM. Figure 2a shows an example of an area of the Mozambique shelf. There, the swIOBC-DBM, constrained solely by multibeam data gives a more realistic representation of the seafloor than GEBCO_14 that displays an artificially undulating seafloor. The same is true for areas of flat, deep seafloor as for example the area of the Mozambique Channel shown in Figure 2b. There, the high-resolution multibeam data, furthermore, show nicely developed sediment waves in the northwest corner.

data, recorded along the tracks of seismic surveys, cover the northern Mozambique Basin. The distribution of the multibeam data however reveals that multibeam coverage is sparse for large parts of the shelf areas and the southern Mozambique Basin (Figure 1b).

The improvements of the swIOBC-DBM, in comparison to GEBCO_14, are particularly obvious in the Mozambique Channel area (Figure 2a). There, a raster of multibeam track-lines is sufficient to characterize the

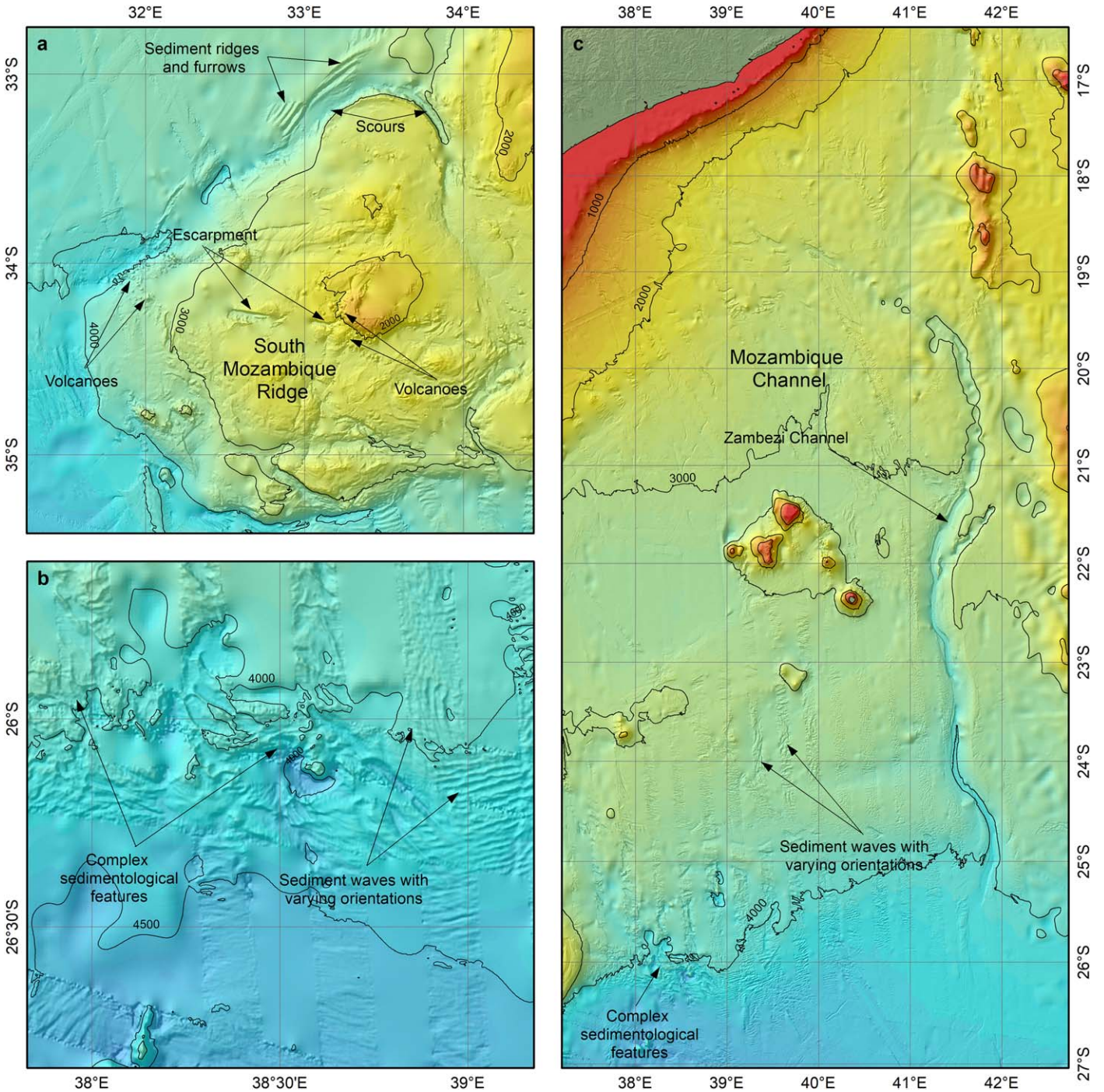

Figure 3. Examples of the swIOBC-DBM. Figure 3a shows the southern Mozambique Ridge with abundant volcanoes, sediment ridges, and scours. In Figure 3b, complex sedimentary and tectonic landforms are displayed. Figure 3c shows sediment waves in the Mozambique Channel and the Zambezi Channel resolved in detail between 41°E and 42°E.

general nature of the seafloor. According to the multibeam data, the seafloor represents mostly a flat plain. This is a contrast to GEBCO_14 that, as a result of using satellite altimetry data in the area, shows an undulating seafloor (Figure 2a). In this area and in areas with similar differences between GEBCO_14 and the multibeam data used in swIOBC-DBM, the interpolated surface between multibeam data represents a more accurate representation of the actual seafloor than GEBCO_14. Therefore, the exclusion of GEBCO_14 data from these areas resulted in an improved representation of the seafloor. This approach is similar to the approach used by Arndt et al. (2013) for the Southern Ocean. By carefully adjusting the areas of large discrepancy, the swIOBC-DBM improved in particular the shelf areas (Figure 2a). In the deep basins, in areas of flat seafloor, the multibeam data also reduced the artificial undulating of GEBCO_14 and added high levels of detail in areas with multibeam coverage (Figure 2b).

A selection of geological and sedimentological features is presented below that can now be observed in the swIOBC. Prominent geological features are kilometer-sized volcanic cones abundant on the southern Mozambique Ridge (Figure 3a), the northwest Agulhas Plateau, and in the northern Agulhas Basin. Some of these volcanoes have already been identified in seismic data by Fischer et al. (2017). To what extent this neo-volcanism (Fischer et al., 2017; Uenzelmann-Neben et al., 1999) can be related to the African Rift system is still under debate (Fischer et al., 2017) and requires further investigations. The swIOBC also images the fault controlled eastern side of the Mozambique Ridge and a large escarpment extending from east to west across the southern Mozambique Ridge (Figure 3a).

In addition to the landforms of geological origin, the swIOBC also reveals a plethora of sedimentological landforms. Sediment waves, scours, sediment ridges, and drifts occur (Figures 1 and 3a–3c) providing information on the interactions of bottom currents on the seafloor over prolonged periods of time indicating areas of erosion, lateral sediment-transport, and deposition (Stow et al., 2002; Uenzelmann-Neben, 2001; Uenzelmann-Neben & Huhn, 2009; Uenzelmann-Neben et al., 2007; Wiles et al., 2014a, 2014b). These landforms have already been described and interpreted by Breitzke et al. (2017) for Mozambique Channel linking them to the flow paths of Antarctic Bottom Water and North Atlantic Deep Water as part of the meridional overturning circulation (Breitzke et al., 2017; Sultan et al., 2007). For the Mozambique, Transkei, and Agulhas Basin, similar analyses are still missing. Other sedimentary landforms in the Mozambique Channel and Basin and the Natal Valley (Figures 3a and 3b) have developed as the result of bottom currents intensified around obstacles on the seafloor (Faugères et al., 1999). In the eastern Natal Valley, where the path of water masses is deferred by the Mozambique Ridge, bottom currents have formed a series of scours and drift sediments (Figure 3a) similar to those described adjacent to the Agulhas Plateau (Uenzelmann-Neben, 2001; Uenzelmann-Neben et al., 2007). In addition, sediment waves on the Mozambique Ridge indicate a potential spillover of waters through the east-west trending valleys of Mozambique Ridge (Figure 3a). In the southern Mozambique Basin, the swIOBC reveals complex crosscutting landforms of varying orientations (Figure 3b) likely representing interactions of tectonic features and bottom currents.

Channels and canyons visible in the swIOBC indicate pathways of focused sediment transport on the African and Madagascan continental slope and in the Mozambique Channel (Figure 1). The most prominent channel system covered by the swIOBC is the Zambezi Channel (Figures 1 and 3c). This prominent feature within the central Mozambique Channel is now better constrained by the swIOBC. It highlights the complex geomorphological details of the Zambezi Channel that set it apart from other low-latitude submarine channels. Zambezi Channel appears more comparable to high-latitude systems controlled by the sporadic influx of sediment laden melt waters (Wiles et al., 2017). A landward continuation of the Zambezi Cannel across the East African continental slope and shelf cannot be identified in the swIOBC (Figures 1 and 3c). In summary, the new high-resolution swIOBC shows details of the seafloor that have been unresolved before, thus providing basic information for future studies.

4. Conclusions

The swIOBC uses the current most comprehensive database of multibeam and singlebeam data to picture the bathymetry of the southwest Indian Ocean in highest detail that again provide important base information for a variety of scientific approaches. Because of the increased resolution (250 m) in areas of multibeam data coverage, sedimentary landforms are now visible and larger submarine features are resolved in more detail. In addition, the swIOBC-DBM gives an indication how improved maps of the seafloor can foster

scientific knowledge. Nevertheless, large areas of the southwest Indian Ocean still lack high-resolution multibeam coverage. Concerted efforts in the future hold the potential to further increase data coverage. Full coverage maps would then allow for quantitative geo-morphological analyses of seafloor landforms as for example comprehensive mapping of the sediment waves in the southwest Indian Ocean. A data set like this provides proxy-information on past and recent bottom current directions and intensities. In this regard, we would like to stress that regional compilations represent ongoing efforts that live from the contribution of the international seafloor mapping community. Consequently, the swIOBC supports the Nippon Foundation-GEBCO Seabed 2030 Project and will be included in GEBCO to improve our knowledge of the world's oceans.

Acknowledgments
We thank all data providers for supporting the swIOBC project. In particular, we would like to thank Cécile Pertuisot from IFREMER for providing the following data: IFREMER 2002 – Data collected by IFREMER/IPGP/CEA – MD 125/SWIFT BIS-CARHOT campaign – *RV Marion Dufresne* and Volkmar Leimer from the BSH for providing multibeam data collected by German research vessels. Multibeam data collection was possible during the *RV Sonne* expeditions AISTEK1 SO182 (grant 03G0182A), AISTEK2 SO183 (grant 03G0183A), MOCOM SO230 (grant 03G0230A), PAGE_Four SO231 (grant 03G0231A&B), and SLIP SO232 (grant 03G0232A) and *RV Pelagia* expedition AISTEK3 (grant 03G0730A). The Captains and crew of each research cruise are thanked for their expert assistance and support over 42 successful cruises. We are grateful to Thierry Schmitt and Rochelle Wigley for reviewing the manuscript and providing helpful comments. Finally, yet importantly, we would like to thank all seafloor mappers providing data to public databases thus helping to get a better look at our planet. The new swIOBC-DBM, the SID and corresponding metadata of this study are available for download from the PANGAEA database at https://doi.org/10.1594/PANGAEA.880618.

References

Arndt, J. E., Schenke, H. W., Jakobsson, M., Nitsche, F. O., Buys, G., Goleby, B., et al. (2013). The International Bathymetric Chart of the Southern Ocean (IBCSO) Version 1.0—A new bathymetric compilation covering circum-Antarctic waters. *Geophysical Research Letters*, *40*, 3111–3117. https://doi.org/10.1002/grl.50413

Breitzke, M., Wiles, E. A., Krocker, R., Watkeys, M. K., & Jokat, W. (2017). Seafloor morphology in the Mozambique Channel: Evidence for long-term persistent bottom-current flow and deep-reaching eddy activity. *Marine Geophysical Research*, *38*(3), 241–269. https://doi.org/10.1007/s11001-017-9322-7

Davies, T. A., Kidd, R. B., & Ramsay, A. T. S. (1995). A time-slice approach to the history of Cenozoic sedimentation in the Indian Ocean. *Sedimentary Geology*, *96*(1–2), 157–179. https://doi.org/10.1016/0037-0738(94)00131-D

de Ruijter, W. P. M., Biastoch, A., Drijfhout, S. S., Lutjeharms, J. R. E., Matano, R. P., Pichevin, T., et al. (1999). Indian-Atlantic interocean exchange: Dynamics, estimation and impact. *Journal of Geophysical Research*, *104*(C9), 20885–20910. https://doi.org/10.1029/1998JC900099

Eagles, G., & König, M. (2008). A model of plate kinematics in Gondwana breakup. *Geophysical Journal International*, *173*(2), 703–717. https://doi.org/10.1111/j.1365-246X.2008.03753.x

Faugères, J.-C., Stow, D. A. V., Imbert, P., & Viana, A. R. (1999). Seismic features diagnostic of contourite drifts. *Marine Geology*, *162*(1), 1–38. https://doi.org/10.1016/S0025-3227(99)00068-7

Fischer, M. D., Uenzelmann-Neben, G., Jacques, G., & Werner, R. (2017). The Mozambique Ridge: A document of massive multistage magmatism. *Geophysical Journal International*, *208*(1), 449–467. https://doi.org/10.1093/gji/ggw403

Gaina, C., Torsvik, T. H., van Hinsbergen, D. J. J., Medvedev, S., Werner, S. C., & Labails, C. (2013). The African Plate: A history of oceanic crust accretion and subduction since the Jurassic. *Tectonophysics*, *604*, 4–25. https://doi.org/10.1016/j.tecto.2013.05.037

Gohl, K., & Uenzelmann-Neben, G. (2001). The crustal role of the Agulhas Plateau, southwest Indian Ocean: Evidence from seismic profiling. *Geophysical Journal International*, *144*(3), 632–646. https://doi.org/10.1046/j.1365-246x.2001.01368.x

Gohl, K., Uenzelmann-Neben, G., & Grobys, N. (2011). Growth and dispersal of a southeast African Large Igneous Province. *South African Journal of Geology*, *114*(3–4), 379–386. https://doi.org/10.2113/gssajg.114.3-4.379

Gordon, A. L. (1986). Interocean exchange of thermocline water. *Journal of Geophysical Research*, *91*(C4), 5037–5046. https://doi.org/10.1029/JC091iC04p05037

Hood, R. R., Beckley, L. E., & Wiggert, J. D. (2017). Biogeochemical and ecological impacts of boundary currents in the Indian Ocean. *Progress in Oceanography*, *156*, 290–325. https://doi.org/10.1016/j.pocean.2017.04.011

Jakobsson, M., Mayer, L., Coakley, B., Dowdeswell, J. A., Forbes, S., Fridman, B., et al. (2012). The International Bathymetric Chart of the Arctic Ocean (IBCAO) Version 3.0. *Geophysical Research Letters*, *39*, L12609. https://doi.org/10.1029/2012GL052219

Jarvis, A., Reuter, H., Nelson, I. A., & Guevara, E. (2008). Hole-filled SRTM for the globe Version 4, available from the CGIAR-CSI SRTM 90m Database. Retrieved from http://srtm.csi.cgiar.org

Jokat, W., Boebel, T., König, M., & Meyer, U. (2003). Timing and geometry of early Gondwana breakup. *Journal of Geophysical Research*, *108*(B9), 2428. https://doi.org/10.1029/2002JB001802

König, M., & Jokat, W. (2010). Advanced insights into magmatism and volcanism of the Mozambique Ridge and Mozambique Basin in the view of new potential field data. *Geophysical Journal International*, *180*(1), 158–180. https://doi.org/10.1111/j.1365-246X.2009.04433.x

Leinweber, V. T., Klingelhoefer, F., Neben, S., Reichert, C., Aslanian, D., Matias, L., et al. (2013). The crustal structure of the Central Mozambique continental margin — Wide-angle seismic, gravity and magnetic study in the Mozambique Channel, Eastern Africa. *Tectonophysics*, *599*, 170–196. https://doi.org/10.1016/j.tecto.2013.04.015

Lutjeharms, J. R. E. (2006). *The Agulhas current*. Berlin, Germany: Springer. https://doi.org/10.1007/3-540-37212-1

Lutjeharms, J. R. E., & Van Ballegooyen, R. C. (1988). The Retroflection of the Agulhas Current. *Journal of Physical Oceanography*, *18*(11), 1570–1583. https://doi.org/10.1175/1520-0485(1988)018<1570:TROTAC>2.0.CO;2

Mayer, L. A., Jakobsson, M., Allen, G. L., Dorschel, B., Falconer, R., Ferrini, V., et al. (2018). The Nippon Foundation—GEBCO Seabed 2030 Project: The quest to see the world's oceans completely mapped by 2030. *Geosciences*, *8*(2), 63. https://doi.org/10.3390/geosciences8020063

Parsiegla, N., Gohl, K., & Uenzelmann-Neben, G. (2008). The Agulhas Plateau: Structure and evolution of a Large Igneous Province. *Geophysical Journal International*, *174*(1), 336–350. https://doi.org/10.1111/j.1365-246X.2008.03808.x

Salman, G., & Abdula, I. (1995). Development of the Mozambique and Ruvuma sedimentary basins, offshore Mozambique. *Sedimentary Geology*, *96*(1–2), 7–41. https://doi.org/10.1016/0037-0738(95)00125-R

Schott, F. A., Dengler, M., & Schoenefeldt, R. (2002). The shallow overturning circulation of the Indian Ocean. *Progress in Oceanography*, *53*(1), 57–103. https://doi.org/10.1016/S0079-6611(02)00039-3

Schott, F. A., & McCreary, J. P., Jr. (2001). The monsoon circulation of the Indian Ocean. *Progress in Oceanography*, *51*(1), 1–123. https://doi.org/10.1016/S0079-6611(01)00083-0

Schott, F. A., Xie, S.-P., & McCreary, J. P., Jr. (2009). Indian Ocean circulation and climate variability. *Reviews of Geophysics*, *47*, RG1002. https://doi.org/10.1029/2007RG000245

Siedler, G., Rouault, M., Biastoch, A., Backeberg, B., Reason, C. J. C., & Lutjeharms, J. R. E. (2009). Modes of the southern extension of the East Madagascar Current. *Journal of Geophysical Research*, *114*, C01005. https://doi.org/10.1029/2008JC004921

Smith, W. H. F., & Sandwell, D. T. (1997). Global sea floor topography from satellite altimetry and ship depth soundings. *Science*, *277*(5334), 1956–1962. https://doi.org/10.1126/science.277.5334.1956

Smith, W. H. F., & Wessel, P. (1990). Gridding with continuous curvature splines in tension. *Geophysics*, *55*(3), 293–305. https://doi.org/10.1190/1.1442837

Stow, D. A. V., Faugères, J.-C., Howe, J. A., Pudsey, C. J., & Viana, A. R. (2002). Bottom currents, contourites and deep-sea sediment drifts: Current state-of-the-art. *Geological Society, London, Memoirs*, *22*(1), 7–20. https://doi.org/10.1144/GSL.MEM.2002.022.01.02.

Sultan, E., Mercier, H., & Pollard, R. T. (2007). An inverse model of the large scale circulation in the South Indian Ocean. *Progress in Oceanography*, *74*(1), 71–94. https://doi.org/10.1016/j.pocean.2007.02.001

Tucholke, B. E., Houtz, R. E., & Barrett, D. M. (1981). Continental crust beneath the Agulhas Plateau, southwest Indian Ocean. *Journal of Geophysical Research*, *86*(B5), 3791–3806. https://doi.org/10.1029/JB086iB05p03791

Uenzelmann-Neben, G. (2001). Seismic characteristics of sediment drifts: An example from the Agulhas Plateau, southwest Indian Ocean. *Marine Geophysical Research*, *22*(5), 323–343. https://doi.org/10.1023/A:1016391314547

Uenzelmann-Neben, G., Gohl, K., Ehrhardt, A., & Seargent, M. (1999). Agulhas Plateau, SW Indian Ocean: New evidence for excessive volcanism. *Geophysical Research Letters*, *26*(13), 1941–1944. https://doi.org/10.1029/1999GL900391

Uenzelmann-Neben, G., & Huhn, K. (2009). Sedimentary deposits on the southern South African continental margin: Slumping versus non-deposition or erosion by oceanic currents? *Marine Geology*, *266*(1–4), 65–79. https://doi.org/10.1016/j.margeo.2009.07.011

Uenzelmann-Neben, G., Schlüter, P., & Weigelt, E. (2007). Cenozoic oceanic circulation within the South African gateway: Indications from seismic stratigraphy. *South African Journal of Geology*, *110*(2–3), 275–294. https://doi.org/10.2113/gssajg.110.2-3.275

van Leeuwen, P. J., de Ruijter, W. P. M., & Lutjeharms, J. R. E. (2000). Natal pulses and the formation of Agulhas rings. *Journal of Geophysical Research*, *105*(C3), 6425–6436. https://doi.org/10.1029/1999JC900196

Weatherall, P., Marks, K. M., Jakobsson, M., Schmitt, T., Tani, S., Arndt, J. E., et al. (2015). A new digital bathymetric model of the world's oceans. *Earth and Space Science*, *2*(8), 331–345. https://doi.org/10.1002/2015EA00010

Wessel, P., Smith, W. H. F., Scharroo, R., Luis, J., & Wobbe, F. (2013). Generic mapping tools: Improved version released. *Eos, Transactions American Geophysical Union*, *94*(45), 409–410. https://doi.org/10.1002/2013EO450001

Wiles, E. A., Green, A., Watkeys, M., Jokat, W., & Krocker, R. (2014a). A new pathway for Deep water exchange between the Natal Valley and Mozambique Basin? *Geo-Marine Letters*, *34*(6), 525–540. https://doi.org/10.1007/s00367-014-0383-1

Wiles, E. A., Green, A., Watkeys, M., Jokat, W., & Krocker, R. (2014b). Anomalous seafloor mounds in the northern Natal Valley, southwest Indian Ocean: Implications for the East African Rift System. *Tectonophysics*, *630*(3), 300–312. https://doi.org/10.1016/j.tecto.2014.05.030

Wiles, E. A., Green, A. N., Watkeys, M. K., & Jokat, W. (2017). Zambezi continental margin: Compartmentalized sediment transfer routes to the abyssal Mozambique Channel. *Marine Geophysical Research*, *38*(3), 227–240. https://doi.org/10.1007/s11001-016-9301-4

Xie, S.-P., Annamalai, H., Schott, F. A., & McCreary, J. P., Jr. (2002). Structure and Mechanisms of South Indian Ocean Climate Variability. *Journal of Climate*, *15*(8), 864–878. https://doi.org/10.1175/1520-0442(2002)015<0864:SAMOSI>2.0.CO;2